# The Doppler effect on indirect detection of decaying dark matter

Devon Powell,[1, 2, *] Ranjan Laha,[1, 2, †] and Tom Abel[1, 2]

[1]*Kavli Institute for Particle Astrophysics and Cosmology (KIPAC),
Department of Physics, Stanford University, Stanford, CA 94305, USA*
[2]*SLAC National Accelerator Laboratory, Menlo Park, CA 94025, USA*
(Dated: September 11, 2016)

[1]

**Introduction:** The search for the particle properties of dark matter is one of the most important research avenues [2–4]. The "weak" interactions experienced by the dark matter particle complicates these searches. Despite decades of multi-pronged searches, we have not yet identified the dark matter particle [5]. One of the most important ways to search for dark matter particles is indirect detection [6].

Due to the enormous astrophysical background, many anomalous signals have been interpreted as a dark matter signal [7–13]. Astrophysical sources such as pulsars or atomic lines are diverse enough to mimic a dark matter signal [14–19]. The separation of signal and background is difficult since one needs to model the background and then find the signal in the same data set. Distinct kinematic signatures arising from dark matter annihilation or decay are used to separate the dark matter signal from background. These signatures include monochromatic photons arising from dark matter annihilation or decay. Past experiences have shown that it is not reliable to only depend on this signature for the identification of a dark matter signal.

In order to better characterize a dark matter signal, Ref. [1] utilized the superb energy resolution, $\sim \mathcal{O}(0.1\%)$, of Hitomi (previously known as Astro-H) to find a new signature. It was shown that our motion around the Galaxy produces a distinct longitudinal dependence in the dark matter signal — a signature of Doppler effect. This new signature is model independent and applicable to any dark matter signal containing a sharp feature. It is unlikely that baryonic phenomenon can produce such a distinct signature [1].

Given the importance of identifying the dark matter particle, it is important to characterize any new model independent signature in detail. We perform such a study in this work using dark matter only simulations from Ref. [20]. As an example of the dark matter signal, we consider the 3.5 keV line [11, 12]. The status of the 3.5 keV line is controversial [21–27]. The malfunctioning of the Hitomi satellite did not permit an observation which would have conclusively tested this signal. We use future Micro-X observations [28] to demonstrate our technique. It is expected that Micro-X will have an energy resolution of 3 eV at 3.5 keV [28], and thus permits dark matter velocity spectroscopy [1]. We emphasize that we are using this 3.5 keV signal as a proxy, and that the underlying physics of this work is model independent.

Any telescope with $\mathcal{O}(0.1\,\%)$ energy resolution can perform dark matter velocity spectroscopy. An improvement in the energy resolution is the natural step in the evolution of telescope instrumentation. This improvement will help in disentangling dark matter signal from background, and improving our knowledge of the astronomical sources. It is a known technology to build detectors with $\mathcal{O}(0.1\%)$ energy resolution, such as INTEGRAL-SPI [29] and Hitomi. Near future instruments like Micro-X [28] and ATHENA [30] will also have a $\mathcal{O}(0.1\%)$ energy resolution.

## Methods:

*Theory:* For a large field of view instrument [28]:

$$\mathcal{F} = \frac{\Gamma}{4\pi\, m_s} \int_\Omega \int_0^\infty d\Omega\, ds\, \rho[r(s,\Omega)]. \tag{1}$$

We can rewrite Eqn. 1 as

$$\frac{d^2\mathcal{F}}{d\Omega\, dE} = \frac{\Gamma}{4\pi\, m_s} \int_0^\infty ds\, \rho[r(s,\Omega)] \frac{dN(E)}{dE}. \tag{2}$$

Similar to the previous paper, we can write

$$\frac{d\tilde{N}(E, r[s,\Omega])}{dE} = \int dE' \frac{dN(E')}{dE'} G(E - E', \sigma_{E'}), \tag{3}$$

where the convolution function $G(E, \sigma_E)$ takes the form of a Gaussian with an width of $\sigma_E = (E/c)\sigma_{v_{\rm LOS}}$. We assume that $\sigma_{v_{\rm LOS}} \approx \sigma_{v_r}(r[s,\Omega])$.

I will now show the derivation of these formulae. Let us assume that the velocity distribution is $f(v)$ and the differential spectrum is $dN/dE = \delta(E - E_0)$. The effect of including this velocity distribution is that it takes the mono energetic spectrum to $\frac{d\tilde{N}}{dE} = \delta\left(E - E_0(1 \pm \frac{v_0}{c})\right)$. From this we can intuitively derive the following formula which is valid for a general $f(v)$:

$$\frac{d\tilde{N}}{dE} = \int f(v) \frac{dN}{dE'} G(E, E')\, dv\, dE' \tag{4}$$

where $G(E, E')$ is the convolution function. To estimate a functional form of $G(E, E')$, we can use the test case $f(v) = \delta(v - v_0)$, and $dN/dE = \delta(E' - E_0)$ to determine $G(E, E') = \delta(E - E'(1 \pm v/c))$.

Let us now consider $f(v) = \frac{1}{\sqrt{2\pi}\sigma_v} e^{v^2/2\,\sigma_v^2}$, so that

$$\frac{d\tilde{N}}{dE} = \int \delta(E' - E_0)\, \frac{1}{\sqrt{2\pi}\sigma}\, e^{v^2/2\,\sigma^2}$$
$$\times\, \delta(E - E'(1 \pm v/c))\, dv\, dE'. \qquad (5)$$

We have $\delta(E - E'(1 \pm v/c)) = \frac{c}{E'}\, \delta\left(v + c - \frac{E}{E'}c\right)$ . We can do the integrals to find

$$\frac{d\tilde{N}}{dE} = \frac{1}{\sqrt{2\pi}}\, \frac{c}{\sigma_v E_0} \exp\left(\frac{-(E - E_0)^2}{2E_0^2\, \sigma_v^2/c^2}\right) \qquad (6)$$

which we can compare with a regular Gaussian to derive $\sigma_E = (E/c)\sigma_v$.

*Simulations:* Our main contribution in this paper is to examine the potential of velocity spectroscopy using more physically realistic N-body simulations, as compared to analytic models using an NFW profile. To this end, we study a suite of Milky Way analogues run using the L-GADGET cosmology code (a descendant of GADGET-2, [31]). These are dark-matter-only zoom-in simulations run by [20] to study subhalo abundance, and their high resolution and multiple realizations makes them suitable for our purposes as well. Each halo has $\mathcal{O}(10^7)$ high-resolution particles with a particle mass $m_p = 4.0 \times 10^5\, \mathrm{M}_\odot$ and total mass $M_{\mathrm{vir}} \simeq 1.2 \times 10^{12}\, \mathrm{M}_\odot$ (note that here, we quote the masses in physical rather than comoving units).



FIG. 1: Halo 374.

While there are 46 realizations available to us, we focus on one halo (labeled Halo 374, see Figure 1) in particular. This halo is the most spherically-symmetric of

the set we studied, with principal axis ratios $b/a = 0.86$ and $c/a = 0.73$. Our reason for this choice is that halo triaxiality actually plays a role in the the symmetry of the significance of the observed signal about the Galactic meridian $\ell = 0°$. However, the presence of a baryonic disk in the Milky Way tends to make the host halo more spherical [32, 33]. As such, we choose to limit ourselves to the more plausible case of Halo 374, while acknowledging the existence of an effect due to triaxiality. We discuss this further in Section .

*Velocity spectroscopy using simulations:* We construct the full spectral intensity seen by the detector directly from the N-body particles, incorporating Doppler shift and velocity dispersion in a straightforward and natural way. This is similar in spirit to both the "sightline" method employed by [34] and the velocity distribution function sampling of [35], both of whom eschew analytic prescriptions in favor of operating directly on the information available in the simulation data.

The procedure for performing velocity spectroscopy on N-body data is relatively straightforward. The density field in an N-body simulation is effectively a sum of Dirac-$\delta$ functions

$$\rho(\mathbf{x}) = \sum_p m_p\, \delta(\mathbf{x} - \mathbf{x}_p)$$

where $\mathbf{x}_p$ and $m_p$ are the position and mass of particle $p$. Integrating this density over a conical field of view $\Omega$ then amounts to a sum over all of the particles within that field of view, $p \in \Omega$, while weighting by the inverse square of the scalar distance to the observer, $r_p^{-2}$.

Analytically integrating (1) using this form for the density field yields the total flux from within the field of view $\Omega$:

$$\mathcal{F} = \frac{\Gamma}{4\pi m_s} \sum_{p \in \Omega} \frac{m_p}{r_p^2} \qquad (7)$$

Likewise, we can integrate (2) to sample the Doppler shifted and broadened observed spectrum:

$$\frac{d\mathcal{F}}{dE} = \frac{\Gamma}{4\pi m_s} \sum_{p \in \Omega} \frac{m_p}{r_p^2}\, \frac{dN[E(1 - v_p/c)]}{dE} \qquad (8)$$

where $v_p$ is the velocity of particle $p$ projected along the line of sight to the observer.

Intuitively, we are "stacking the spectra" from the individual simulation particles, with weights reflecting the $r_p^{-2}$ dependence in the observed flux. One can see that by considering the LOS velocity of each particle independently, we automatically capture the spectral convolution introduced by the bulk velocity dispersion.

We focus here on the special case where $dN/dE$ is a line. In this case, computing the observed spectrum is

then as simple as building a flux-weighted histogram of the line-of-sight velocities for all particles in the sampling cone, though as we will see it is easier to forgo binning and compute the line width directly. See Figure 2 for an illustration.
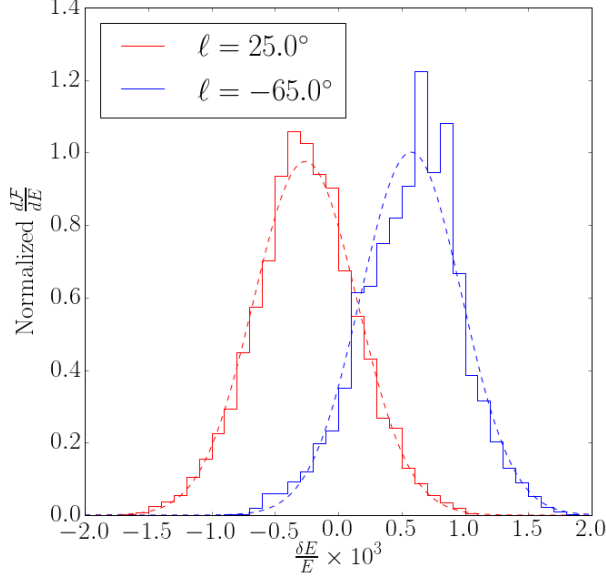


FIG. 2: A comparison of empirical histograms (solid) for the observed line spectrum $d\mathcal{F}/dE$ against their Gaussian models (dashed) as computed using (9) and (10). These were calculated using Micro-X parameters for galactic latitude $b = 25°$ and two galactic latitudes $\ell$. These model spectra give a good fit to the data and allow us to forgo binning in practice.

The flux-weighted mean line-of-sight velocity for a field of view is

$$\langle v \rangle = \frac{1}{\mathcal{F}} \frac{\Gamma}{4\pi m_s} \sum_{p \in \Omega} \frac{m_p}{r_p^2} v_p \qquad (9)$$

It is then easy to see that the mean Doppler shift (the observed shift in the energy of the line) is $\langle \delta E \rangle = (E/c)\langle v \rangle$.

Likewise, we can compute the width of the observed line $\sigma_E$ directly by finding the flux-weighted variance of the line-of-sight velocities $v_p$:

$$\sigma_v^2 = \frac{1}{\mathcal{F}} \frac{\Gamma}{4\pi m_s} \sum_{p \in \Omega} \frac{m_p}{r_p^2} (v_p - \langle v \rangle)^2 \qquad (10)$$

The width of the Doppler-broadened line is then $\sigma_E = (E/c)\sigma_v$. In Figure 2 we show a comparison between this analytic form for the line width and its true histogram.

*Counting uncertainty in the line centroid:* We adopt the same model as [1] when treating the number

counting statistics in the energy of a decay line. The uncertainty in the energy of the line centroid is given by

$$\sigma_{\text{cent}} = (\sigma_E^2 + \sigma_{\text{inst}}^2)^{1/2} \, C(N_s/N_b) \, N_s^{-1/2} \qquad (11)$$

where $\sigma_{\text{inst}}$ is the instrumental uncertainty in energy (corresponding to the spectral resolution), $N_s$ and $N_b$ are the number of signal and background photons, respectively, and $C(R) = \sqrt{1 + 4R}$ is the optimal Cramer-Rao bound [] for the given signal-to-background ratio.

We model $N_b$ using the cosmic X-ray background model of [36],

$$\left(\frac{dN}{dE}\right)_{\text{CXB}} = \frac{C}{(E/E_B)^{\Gamma_1} + (E/E_B)^{\Gamma_2}}$$

where $C = 10.15 \times 10^{-2} \, \text{photons} \, \text{cm}^{-2} \, \text{s}^{-1} \, \text{str}^{-1} \, \text{kev}^{-1}$, $E_B = 29.99 \, \text{keV}$, $\Gamma_1 = 1.32$, and $\Gamma_2 = 2.88$. For the spectral resolution of Micro-X, this yields a background flux at 3.5 keV of .....

We compute the figure of merit...

Integral of the BG flux for a given spectral resolution?

*Micro-X and future observations:*

**Results and discussion:** We present the results of our velocity spectroscopy on Halo 374 with Micro-X parameters in Figure 3. Our main insight is that our analytic model matches the result computed from the N-body simulation extremely well, giving us further confidence in this idealized analytic model after having compared to simulation data.

We find that the pointings $\ell$ centered around $\pm 75°$ exclude $\delta E/E = 0$ with the highest significance, at $\sim 1.5\sigma$. $\ell \sim \pm 75°$ optimizes between two competing effects. The first is the higher J-factor, hence higher photon flux, nearer the Galactic center, giving a smaller uncertainty in the energy of a line detected at small $\ell$. The second is that the mean velocity along the line-of-sight relative to the dark matter increases with $\ell$ (up to $\ell = 90°$), shifting the observed line further from $\delta E/E = 0$.

*Significance of a detection:* While $1.5\sigma$ is certainly not significant enough to claim a detection for a single pointing, there is ample reason to be optimistic about this result. First of all is the fact that the uncertainty in the line centroid scales as $\sigma_{\text{cent}} \propto N_s^{-1/2}$ (see (??)). This further implies that $\sigma_{\text{cent}} \propto t_{\text{exp}}^{-1/2}$. In other words, to achieve a $\sim 6\sigma$ exclusion of $\delta E/E = 0$ one would need an instrument comparable to Micro-X, but simply observe for $\sim 16$ times longer.
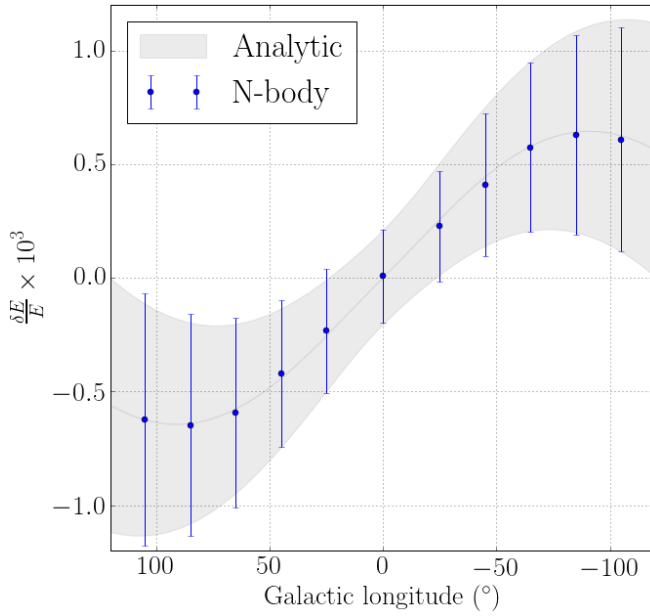
FIG. 3: Velocity spectroscopy of the Milky Way halo, giving the position of the observed line centroid due to sterile neutrino decay as a function of Galactic longitude $\ell$, with latitude $b = 25°$. This compares results as computed from an N-body simulation (Halo 374; see Section ) for the instrumental parameters of Micro-X against our analytic model (Section ), showing good agreement. Note that the error bars and shaded region represent the 1-$\sigma$ uncertainty in the energy of the line centroid, rather than the Doppler-broadened width of the line.

*Halo triaxiality:* Here, we briefly address the fact that halo triaxiality can bias the significance of a detection to the east or west of the galactic center. When observing above the Galactic plane (in this work, $b = 25°$) any ellipticity of the Galactic halo on the sky can give a higher flux to one side of $\ell = 0°$ than the other. While the mean prediciton for the line centroid matches the analytic model for a spherical halo quite well, observing to one side of the GC allows one to exclude $\delta E/E = 0$ with higher significance due to better photon counting statistics. This is illustrated in Figure 5.

**Conclusions:**

————

* dmpowel1@stanford.edu
† rlaha@stanford.edu



(a) Flux.



(b) Doppler-shifted line centroid.



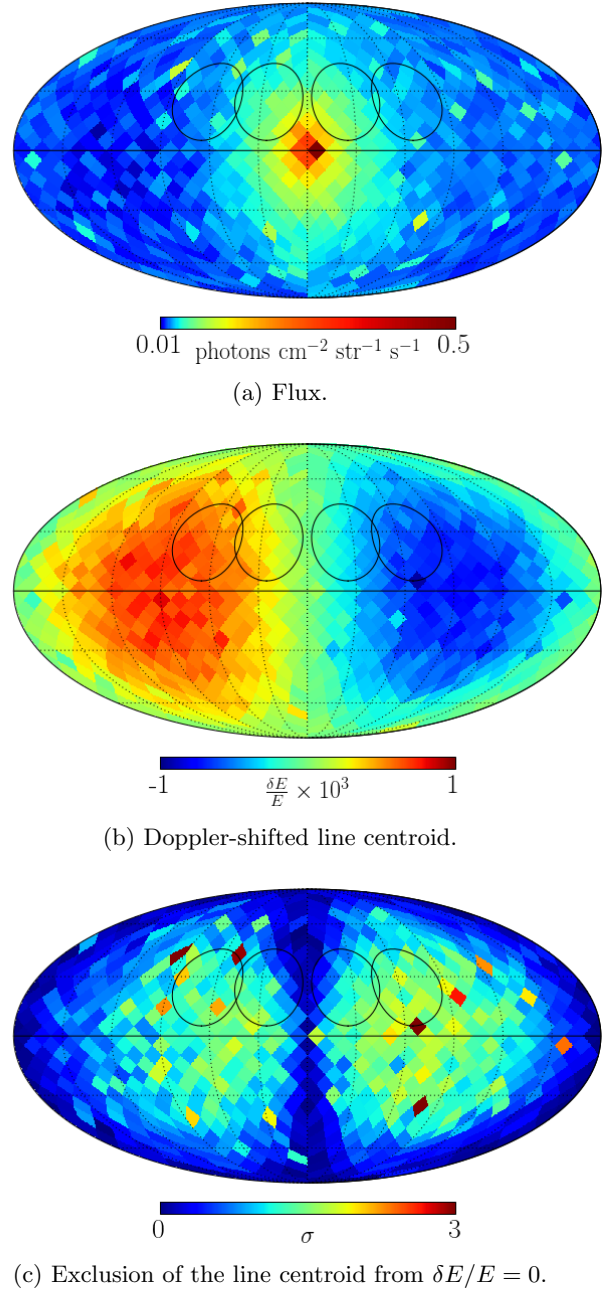(c) Exclusion of the line centroid from $\delta E/E = 0$.

FIG. 4: Sky maps illustrating the principle of velocity spectroscopy. Top: The flux map. Middle: The dipole pattern in the line energy induced by our motion relative to the Milky Way halo. Bottom: The signicance of the detection of Doppler shifting of a dark matter decay line, indicating the number of $\sigma$ by which $\delta E/E = 0$ can be excluded for a Micro-X-like observation. Black circles indicate the FOV of Micro-X on the sky for four pointings.

[1] E. G. Speckhard, K. C. Y. Ng, J. F. Beacom, and R. Laha, "Dark Matter Velocity Spectroscopy", *Physical Review Letters* **116** (2016), no. 3, 031301,
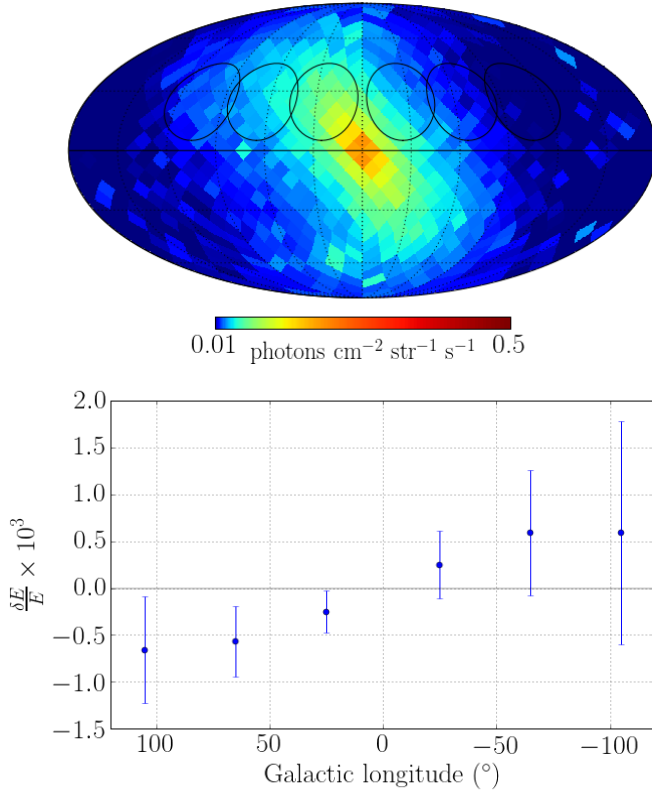
FIG. 5: Asymmetry of the Milky Way halo (here, Halo 800 with $b/a =$ and $c/a =$) could skew the significance of the observed signal to the east or west. Each field of view (black circles in the sky map) corresponds to a data point in the lower plot.

arXiv:1507.04744.

[2] G. Jungman, M. Kamionkowski, and K. Griest, "Supersymmetric dark matter", *Phys. Rept.* **267** (1996) 195–373, arXiv:hep-ph/9506380.

[3] G. Bertone, D. Hooper, and J. Silk, "Particle dark matter: Evidence, candidates and constraints", *Phys. Rept.* **405** (2005) 279–390, arXiv:hep-ph/0404175.

[4] L. E. Strigari, "Galactic Searches for Dark Matter", *Phys. Rept.* **531** (2013) 1–88, arXiv:1211.7090.

[5] G. Bertone and D. Hooper, "A History of Dark Matter", *Submitted to: Rev. Mod. Phys.*, 2016 arXiv:1605.04909.

[6] M. Klasen, M. Pohl, and G. Sigl, "Indirect and direct search for dark matter", *Prog. Part. Nucl. Phys.* **85** (2015) 1–32, arXiv:1507.03800.

[7] K. N. Abazajian, N. Canac, S. Horiuchi, M. Kaplinghat, and A. Kwa, "Discovery of a New Galactic Center Excess Consistent with Upscattered Starlight", *JCAP* **1507** (2015), no. 07, 013, arXiv:1410.6168.

[8] T. Daylan, D. P. Finkbeiner, D. Hooper, T. Linden, S. K. N. Portillo, N. L. Rodd, and T. R. Slatyer, "The characterization of the gamma-ray signal from the central Milky Way: A case for annihilating dark matter", *Phys. Dark Univ.* **12** (2016) 1–23, arXiv:1402.6703.

[9] S. K. Lee, M. Lisanti, B. R. Safdi, T. R. Slatyer, and W. Xue, "Evidence for Unresolved $\gamma$-Ray Point Sources in the Inner Galaxy", *Phys. Rev. Lett.* **116** (2016), no. 5, 051103, arXiv:1506.05124.

[10] R. Bartels, S. Krishnamurthy, and C. Weniger, "Strong support for the millisecond pulsar origin of the Galactic center GeV excess", *Phys. Rev. Lett.* **116** (2016), no. 5, 051102, arXiv:1506.05104.

[11] E. Bulbul, M. Markevitch, A. Foster, R. K. Smith, M. Loewenstein, and S. W. Randall, "Detection of An Unidentified Emission Line in the Stacked X-ray spectrum of Galaxy Clusters", *Astrophys. J.* **789** (2014) 13, arXiv:1402.2301.

[12] A. Boyarsky, O. Ruchayskiy, D. Iakubovskyi, and J. Franse, "Unidentified Line in X-Ray Spectra of the Andromeda Galaxy and Perseus Galaxy Cluster", *Phys. Rev. Lett.* **113** (2014) 251301, arXiv:1402.4119.

[13] O. Urban, N. Werner, S. W. Allen, A. Simionescu, J. S. Kaastra, and L. E. Strigari, "A Suzaku Search for Dark Matter Emission Lines in the X-ray Brightest Galaxy Clusters", *Mon. Not. Roy. Astron. Soc.* **451** (2015), no. 3, 2447–2461, arXiv:1411.0050.

[14] R. M. O'Leary, M. D. Kistler, M. Kerr, and J. Dexter, "Young Pulsars and the Galactic Center GeV Gamma-ray Excess", arXiv:1504.02477.

[15] T. D. Brandt and B. Kocsis, "Disrupted Globular Clusters Can Explain the Galactic Center Gamma Ray Excess", *Astrophys. J.* **812** (2015), no. 1, 15, arXiv:1507.05616.

[16] R. M. O'Leary, M. D. Kistler, M. Kerr, and J. Dexter, "Young and Millisecond Pulsar GeV Gamma-ray Fluxes from the Galactic Center and Beyond", arXiv:1601.05797.

[17] L. Gu, J. Kaastra, A. J. J. Raassen, P. D. Mullen, R. S. Cumbee, D. Lyons, and P. C. Stancil, "A novel scenario for the possible X-ray line feature at 3.5 keV: Charge exchange with bare sulfur ions", *Astron. Astrophys.* **584** (2015) L11, arXiv:1511.06557.

[18] K. J. H. Phillips, B. Sylwester, and J. Sylwester, "The X-ray line feature at 3.5 keV in galaxy cluster spectra", *Astrophys. J.* **809** (2015) 50.

[19] C. Shah, S. Dobrodey, S. Bernitt, R. Steinbrugge, J. R. C. Lopez-Urrutia, L. Gu, and J. Kaastra, "Laboratory measurements compellingly support charge-exchange mechanism for the 'dark matter' ~3.5 keV X-ray line", arXiv:1608.04751.

[20] Y.-Y. Mao, M. Williamson, and R. H. Wechsler, "The Dependence of Subhalo Abundance on Halo Concentration", *Astrophys. J.* **810** (2015) 21, arXiv:1503.02637.

[21] D. Iakubovskyi, "Observation of the new emission line at 3.5 keV in X-ray spectra of galaxies and galaxy clusters", arXiv:1510.00358.

[22] T. E. Jeltema and S. Profumo, "Deep XMM Observations of Draco rule out at the 99% Confidence Level a Dark Matter Decay Origin for the 3.5 keV Line", *Mon. Not. Roy. Astron. Soc.* **458** (2016), no. 4, 3592–3596, arXiv:1512.01239.

[23] O. Ruchayskiy, A. Boyarsky, D. Iakubovskyi, E. Bulbul, D. Eckert, J. Franse, D. Malyshev, M. Markevitch, and A. Neronov, "Searching for decaying dark matter in deep XMM-Newton observation of the Draco dwarf spheroidal", *Mon. Not. Roy. Astron. Soc.* **460** (2016), no. 2, 1390–1398, arXiv:1512.07217.

[24] E. Bulbul, M. Markevitch, A. Foster, E. Miller, M. Bautz, M. Loewenstein, S. W. Randall, and R. K.

Smith, "Searching for the 3.5 keV Line in the Stacked Suzaku Observations of Galaxy Clusters", arXiv:1605.02034.

[25] **Hitomi** Collaboration, F. A. Aharonian *et al.*, "Hitomi constraints on the 3.5 keV line in the Perseus galaxy cluster", arXiv:1607.07420.

[26] F. Hofmann, J. S. Sanders, K. Nandra, N. Clerc, and M. Gaspari, "7.1 keV sterile neutrino constraints from X-ray observations of 33 clusters of galaxies with Chandra ACIS", *Astron. Astrophys.* **592** (2016) A112, arXiv:1606.04091.

[27] J. P. Conlon, F. Day, N. Jennings, S. Krippendorf, and M. Rummel, "Consistency of Hitomi, XMM-Newton and Chandra 3.5 keV data from Perseus", arXiv:1608.01684.

[28] **XQC** Collaboration, E. Figueroa-Feliciano *et al.*, "Searching for keV Sterile Neutrino Dark Matter with X-ray Microcalorimeter Sounding Rockets", *Astrophys. J.* **814** (2015), no. 1, 82, arXiv:1506.05519.

[29] D. Attie *et al.*, "INTEGRAL/SPI ground calibration", *Astronomy and Astrophysics* **411** (2003) L71–L79, arXiv:astro-ph/0308504.

[30] D. Barret *et al.*, "The Athena X-ray Integral Field Unit (X-IFU)", arXiv:1608.08105.

[31] V. Springel, "The cosmological simulation code GADGET-2", *M.N.R.A.S.* **364** (2005) 1105–1134, arXiv:astro-ph/0505010.

[32] V. P. Debattista, B. Moore, T. Quinn, S. Kazantzidis, R. Maas, L. Mayer, J. Read, and J. Stadel, "The Causes of Halo Shape Changes Induced by Cooling Baryons: Disks versus Substructures", *Astrophys. J.* **681** (2008) 1076–1088, arXiv:0707.0737.

[33] S. E. Bryan, S. T. Kay, A. R. Duffy, J. Schaye, C. Dalla Vecchia, and C. M. Booth, "The impact of baryons on the spins and shapes of dark matter haloes", *M.N.R.A.S.* **429** (2013) 3316–3329, arXiv:1207.4555.

[34] M. R. Lovell, G. Bertone, A. Boyarsky, A. Jenkins, and O. Ruchayskiy, "Decaying dark matter: the case for a deep X-ray observation of Draco", *M.N.R.A.S.* **451** (2015) 1573–1585, arXiv:1411.0311.

[35] Y.-Y. Mao, L. E. Strigari, R. H. Wechsler, H.-Y. Wu, and O. Hahn, "Halo-to-halo Similarity and Scatter in the Velocity Distribution of Dark Matter", *Astrophys. J.* **764** (2013) 35, arXiv:1210.2721.

[36] M. Ajello, J. Greiner, G. Sato, D. R. Willis, G. Kanbach, A. W. Strong, R. Diehl, G. Hasinger, N. Gehrels, C. B. Markwardt, and J. Tueller, "Cosmic X-Ray Background and Earth Albedo Spectra with Swift BAT", *Astrophys. J.* **689** (2008) 666–677, arXiv:0808.3377.